Core conditions of high- and low-adiabat OMEGA implosions via x-ray spectroscopy

R. Florido[1,2], T. Nagayama[1], R. C. Mancini[1], R. Tommasini[3], J. Delettrez[4], S. Regan[4], V. Smalyuk[4], R. Rodríguez[2], J.M. Gil[2]

[1] Department of Physics, University of Nevada, Reno (USA)
[2] Departamento de Física, Universidad de Las Palmas de Gran Canaria, Las Palmas de Gran Canaria (Spain)
[3] Lawrence Livermore National Laboratory, Livermore (USA)
[4] Laboratory for Laser Energetics, University of Rochester, New York (USA)

Direct-drive, high- and low-adiabat OMEGA implosions

Overview

- **High adiabat:** 1ns square laser pulse shape, 23kJ UVOT
  Low adiabat: α2/α3 laser pulse shapes, 18kJ/20kJ UVOT
- **Plastic shells:**
  Initial radius: R_0 = 408 μm (h.a.) / 400 μm (l.a.)
  Wall thickness: d = 27 μm
  Filling pressure: 20 atm of D_2 + 0.07 atm of Ar
  Ar tracer is added for spectroscopic diagnostics
- **Two streaked X-ray spectrometers:**
  SSC1 low-speed (150ps/mm) and SSCA high-speed (50ps/mm) record time-resolved, space-integrated argon K-shell line spectra.
  Spectral resolution power $\lambda/\Delta\lambda \approx 500$

Direct-drive, high- and low-adiabat OMEGA implosions

Example of SSC1 image

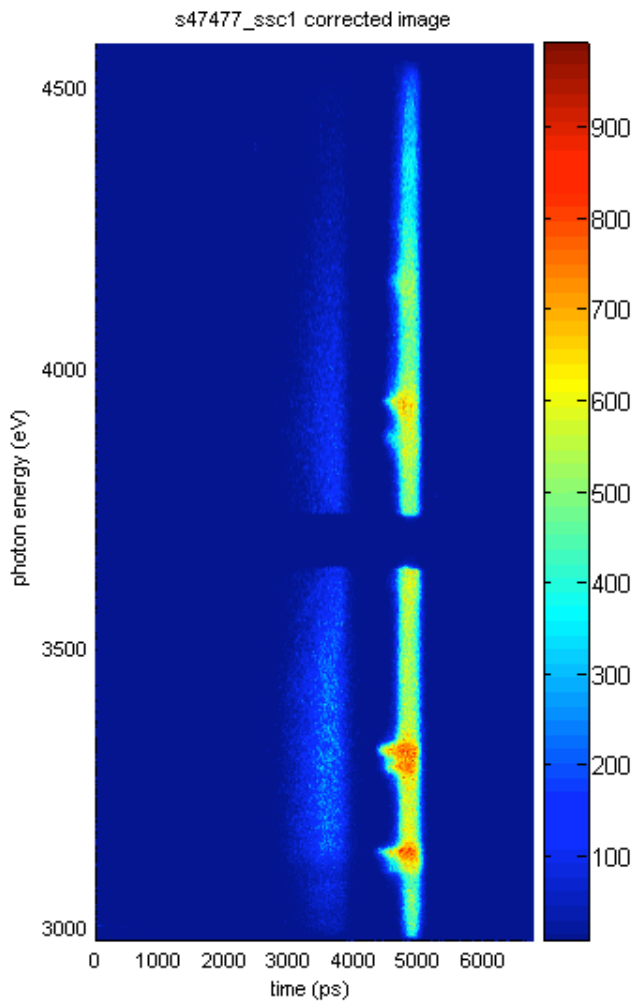

Example of SSCA image

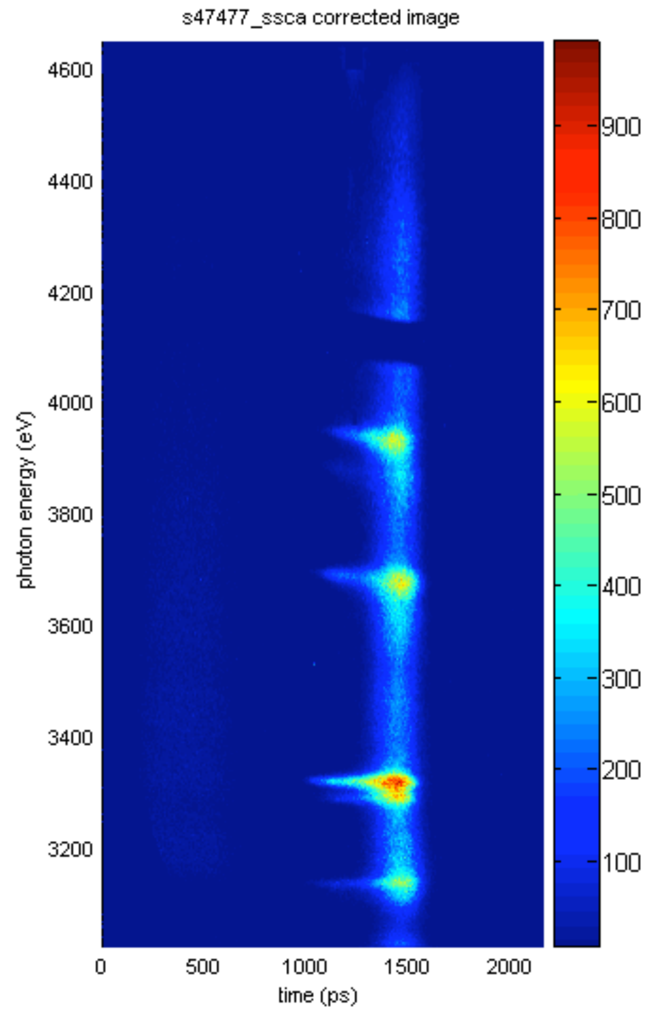

Direct-drive, high- and low-adiabat OMEGA implosions

- The observed spectra includes the Heα, Lyα, Heβ, Heγ, Lyβ and Lyγ line emissions as well as their associated He- and Li-like satellites thus covering a broad photon energy range from 3100 eV to 4200 eV.

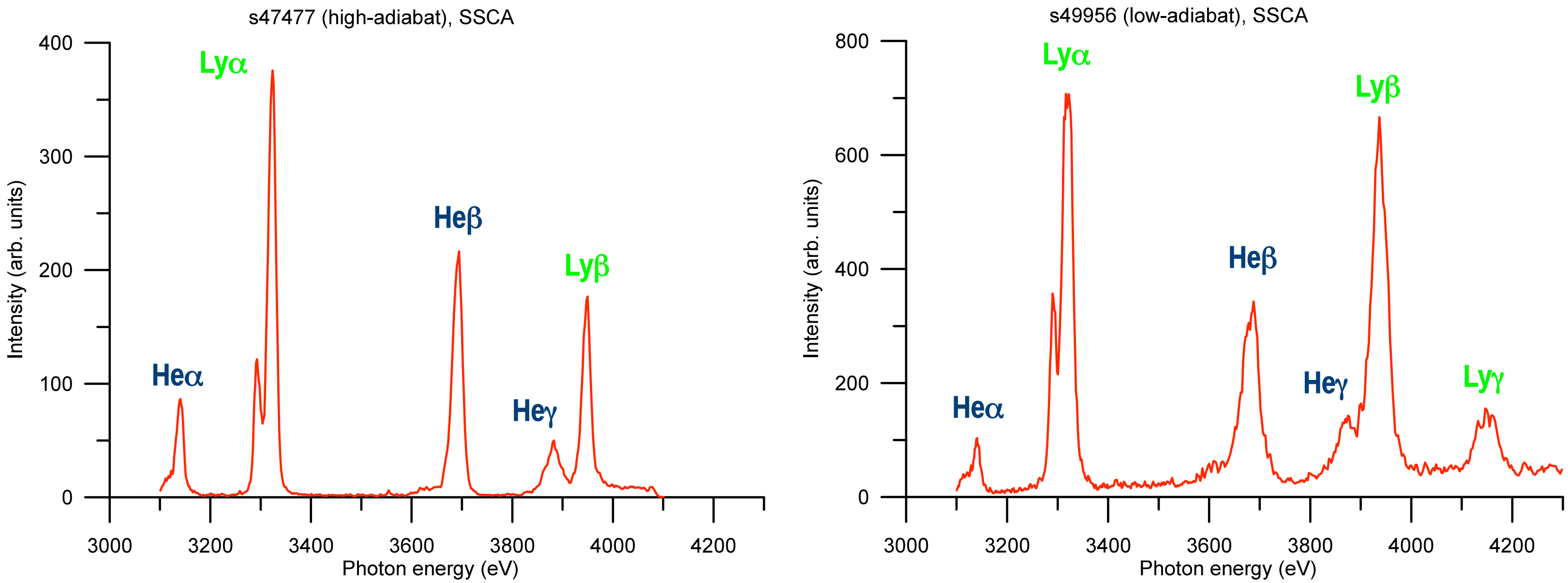

- In addition, three identical DDMMI narrow-band x-ray imagers record gated, narrow-band core images based on Ar K-shell line emission: Lyα, Heβ and Lyβ (see Nagayama poster)

Data processing

- An IDL GUI was built [2] to objectively work with the time and energy scale calibration and to make the extraction of vertical or horizontal selections over the image.
- A vertical or horizontal selection allows to extract a spectral lineout or time history, respectively.

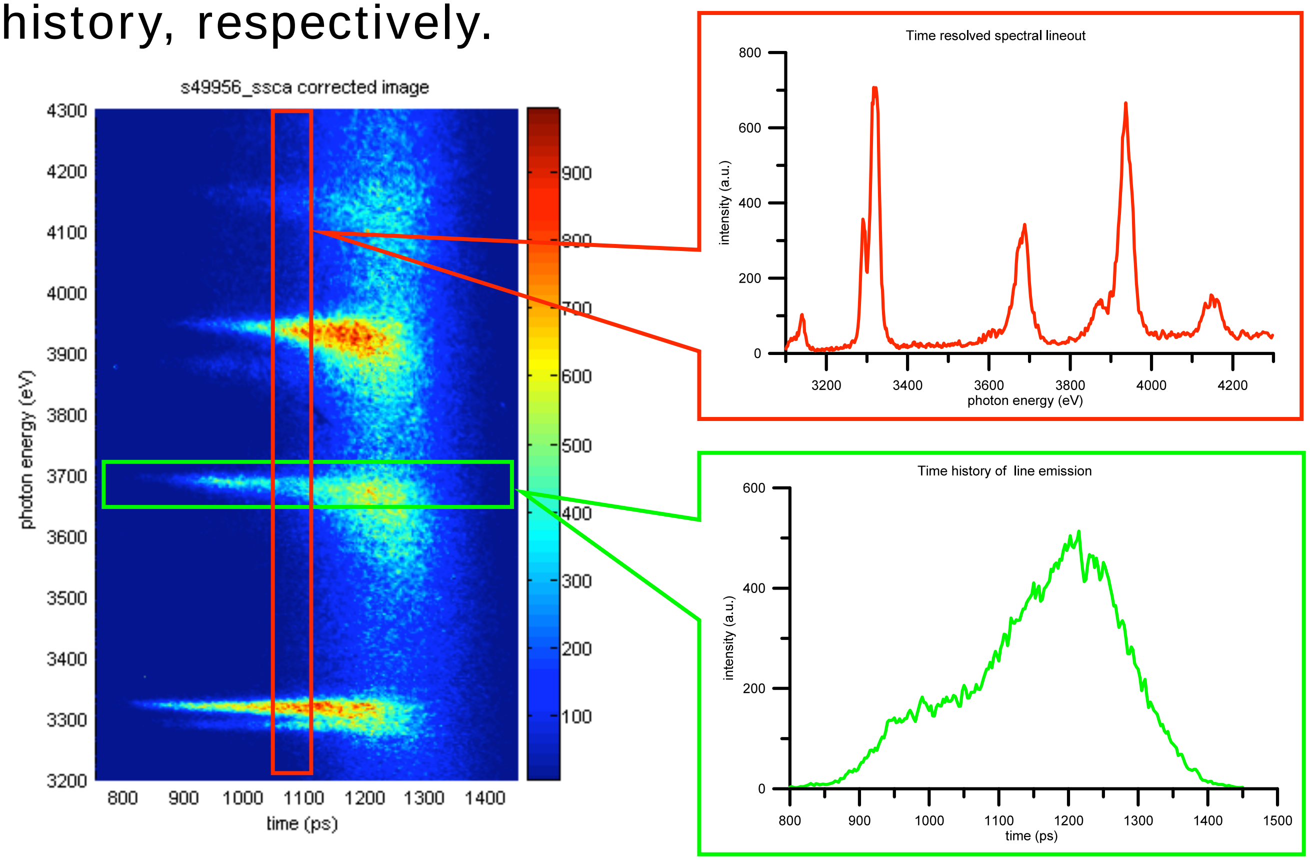

Data processing

- Streaked spectra were corrected for variations in x-ray spectral sensitivity and streak camera flat fielding effects using the photometrically calibrated spectra of a time-integrated spectrometer.
- X-ray continuum emission from an undoped capsule was measured with a time-integrated spectrometer. Then streaked spectrum from an implosion with no Ar was integrated in time and compared with the x-ray continuum emission. The ratio of this two quantities is the photometric calibration [1]. Finally, this calibration is applied to each time-resolved spectrum.

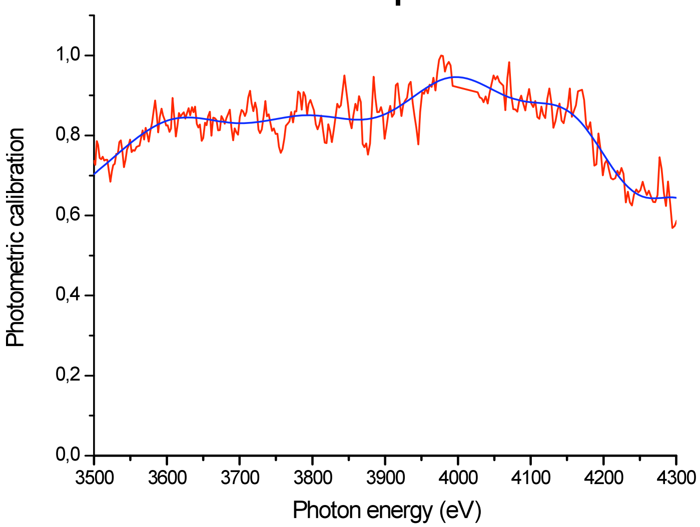

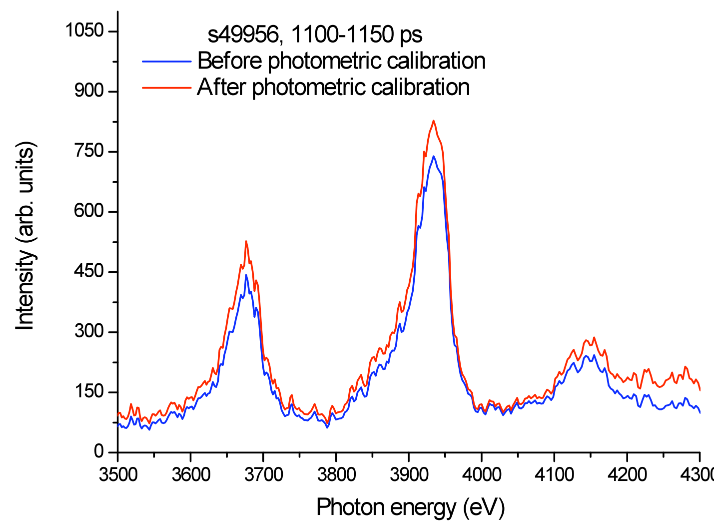

Data processing

- For each time-resolved spectrum, the x-ray continuum emission in the photon energy range of analysis is fitted in the measured spectrum and then subtracted from it, prior comparison with the modeled Ar spectra (which includes line and radiative recombination emissions).

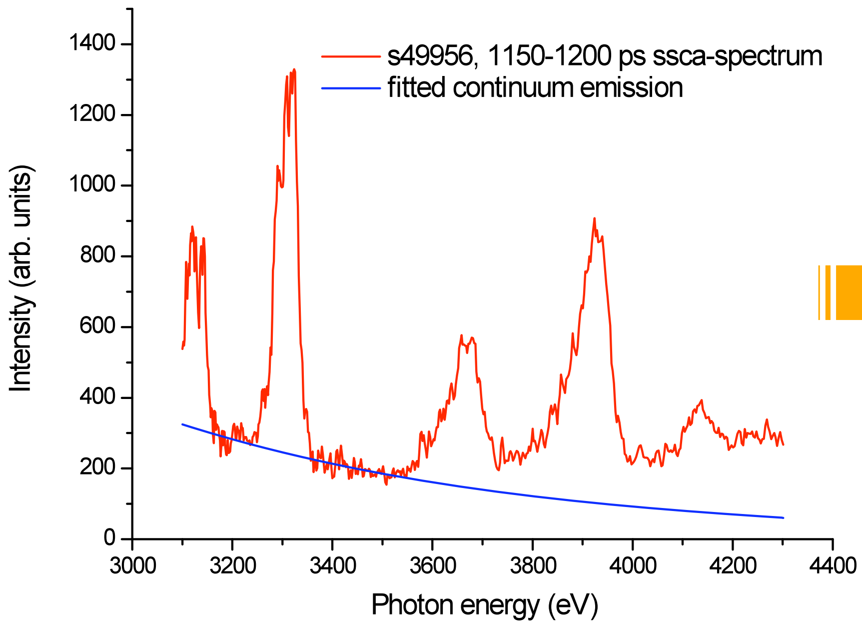

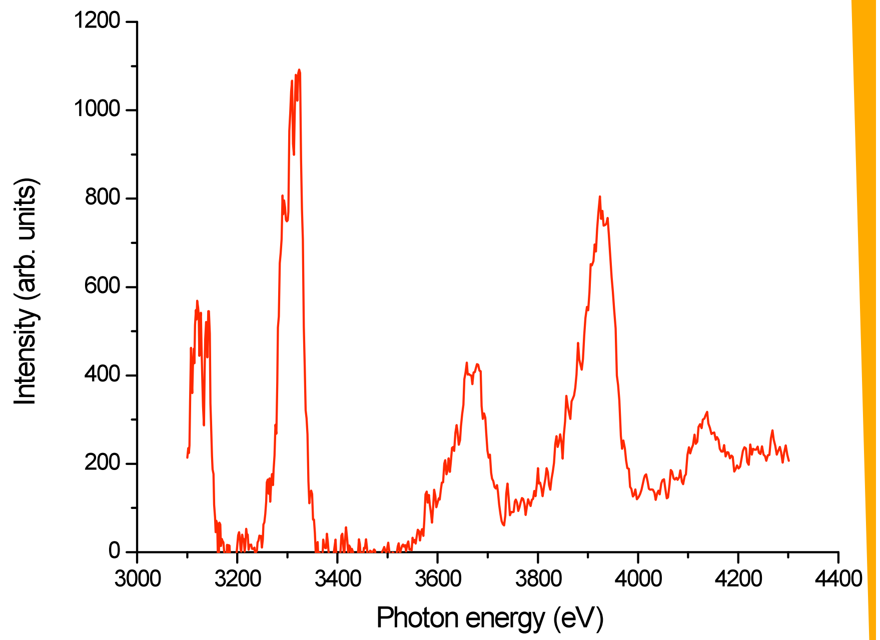

Atomic kinetic model and code: ABAKO

General remarks

- Theoretical calculations have been done using the collisional-radiative atomic kinetics code **ABAKO** [3]. Some of its more remarkable capabilities are:

Versatility

- Plasmas of any *Z* element can be studied.
- It applies over a wide range of temperatures and densities.
- Optically thin and optically thick cases are considered.

Compromise between accuracy & computational cost

- ABAKO assembles a set of simple analytical models which yield substantial savings of computer resources. Yet still providing good comparisons with more elaborated codes and models.
- Here we apply it to detailed spectroscopic analysis.

Atomic kinetic model and code: ABAKO

ABAKO flowchart

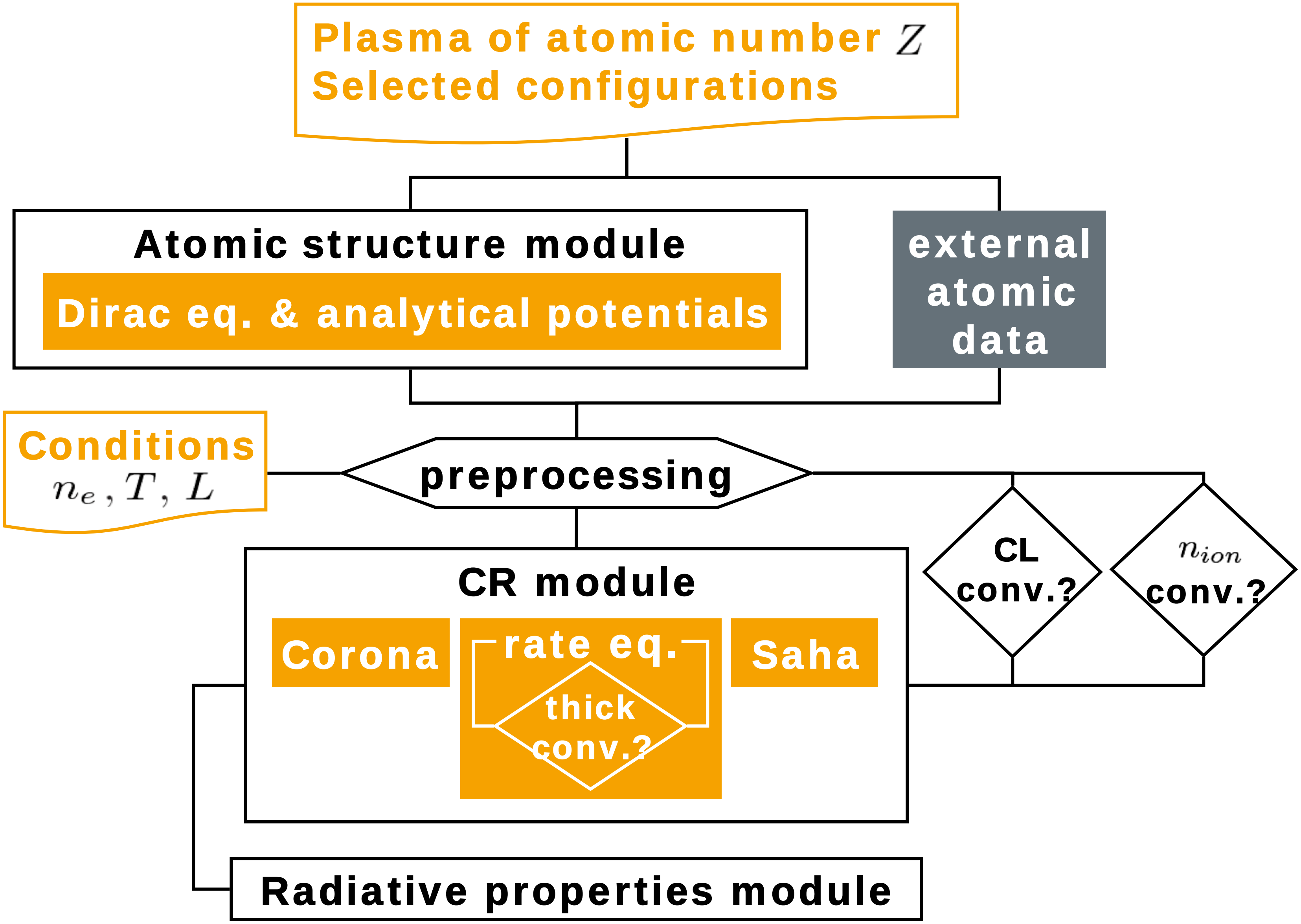

Atomic kinetic model and code: ABAKO

CR module

- Steady-state rate equations are solved to find out the level populations

$$\sum_{\zeta' m'} N_{\zeta' m'}(\mathbf{r})\,\mathbb{R}^{+}_{\zeta' m' \to \zeta m} - \sum_{\zeta' m'} N_{\zeta m}(\mathbf{r})\,\mathbb{R}^{-}_{\zeta m \to \zeta' m'} = 0$$

- No radiation-driven processes are explicitly considered.

Atomic process	Rate coefficient	Expression
spontaneous decay	$\mathcal{A}_{\zeta j \to \zeta i}$	*Einstein*
collisional excitation	$\mathcal{E}_{\zeta i \to \zeta j}$	*Van Regemorter*
collisional deexcitation	$\mathcal{D}_{\zeta j \to \zeta i}$	detailed balance
radiative recombination	$\mathcal{R}^{r}_{\zeta+1 j \to \zeta i}$	*Kramers*
collisional ionization	$\mathcal{I}_{\zeta i \to \zeta+1 j}$	*Lotz*
three-body recombination	$\mathcal{R}^{3}_{\zeta+1 j \to \zeta i}$	detailed balance
autoionization	$\mathcal{A}u_{\zeta i \to \zeta+1 j}$	detailed balance
electron capture	$\mathcal{C}_{\zeta+1 j \to \zeta i}$	ABAKO approach

Atomic kinetic model and code: ABAKO

CR module

- **Autoionization and electron capture:** A proper adaptation of a known approximation [4] allows ABAKO to include autoionizing states explicitly. The electron capture cross-section is approximated by the collisional excitation cross-section.

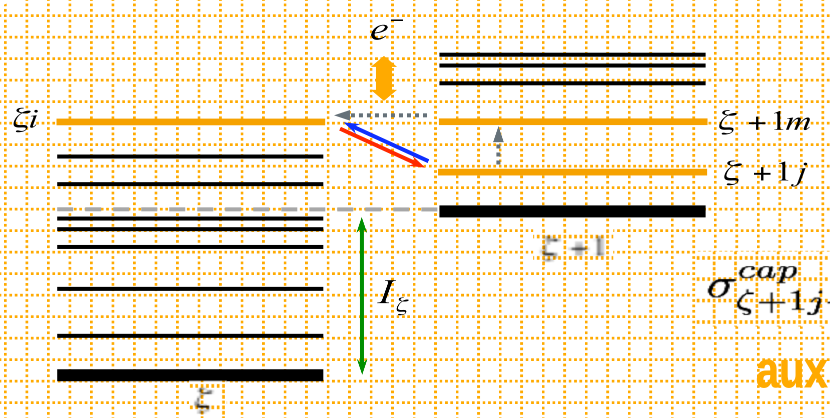

Schematic description of autoionization and electron capture processes.

$$\sigma^{cap}_{\zeta+1j\rightarrow\zeta i}(\varepsilon) \approx \sigma^{exc}_{\zeta+1j\rightarrow\zeta+1m}(\varepsilon)$$

auxiliary state $\zeta+1m$

- **Escape factor formalism** [5] for basic geometries –plane, cylindrical and spherical- is used to take into account **bound-bound opacity effects**

- **Lowering of the ionization potencial** is taken into account following the Stewart & Pyatt formalism [6].

Atomic kinetic model and code: ABAKO

Additional features

- Some additional features have been included for the analysis of spectra from direct-drive implosions.

To determine the population distribution:

- Extension from mono to multicomponent plasmas was necessary to deal with the argon-deuterium mixture.
- We used a semiempirical formula for estimation of Stark widths [7]. Natural, Stark and Doppler broadenings are taken into account in the context of Voigt line profiles.

To determine the synthetic spectrum:

- A database of detailed Stark broadened line shapes [8,9], including the effects of plasma microfields due to electrons and ions, was used to compute the theoretical spectrum.
- According with [10], a proper calculation of the flux of emergent radiation in a spherical and uniform medium was also implemented.

Atomic kinetic model and code: ABAKO

Additional features

To determine the synthetic spectrum:

- To model the emergent intensity in the higher photon energy range several **radiative recombination emissions** has been included in the theoretical spectrum:
  - From full-stripped to H-like ground state.
  - From H-like ground state to He-like ground state.
  - From *nl* H-like excited states to 1s*nl* He-like excited states, up to $n=4$.
- To compute the radiative recombination emission, an analytical fit of the photoionization cross-section was performed for each case over a quantum-mechanical calculation provided by LANL suite of codes.

Atomic kinetic model and code: ABAKO

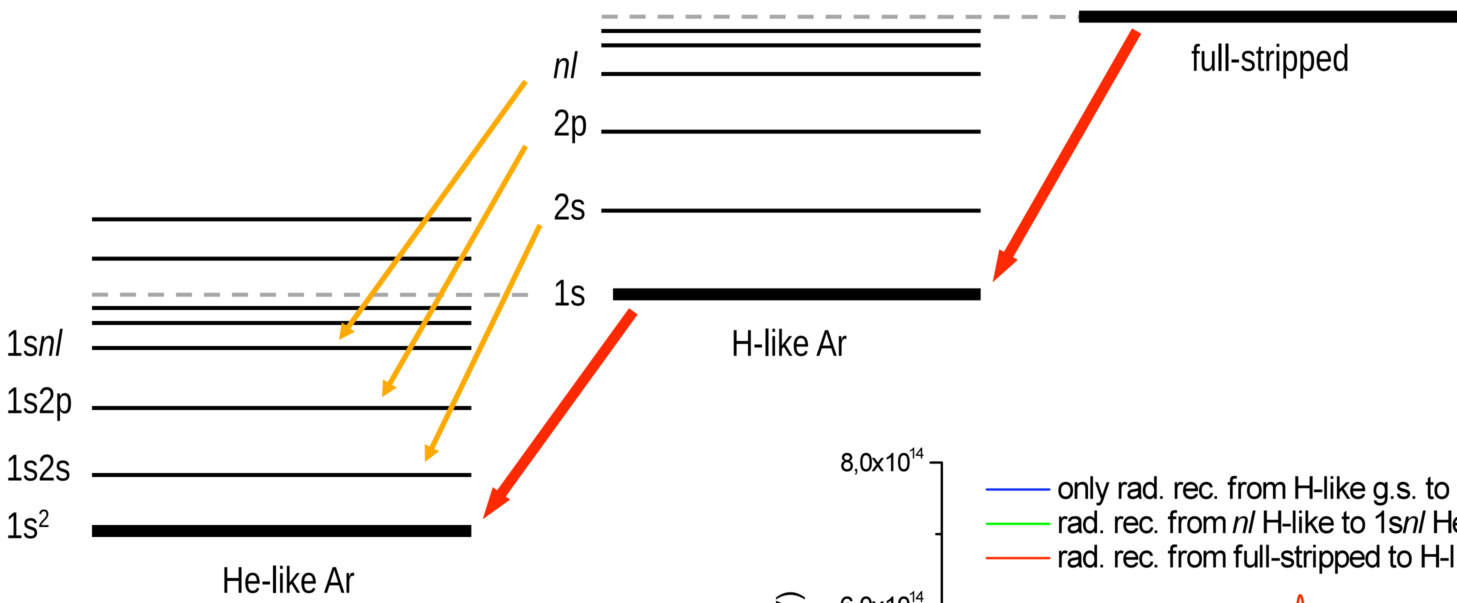

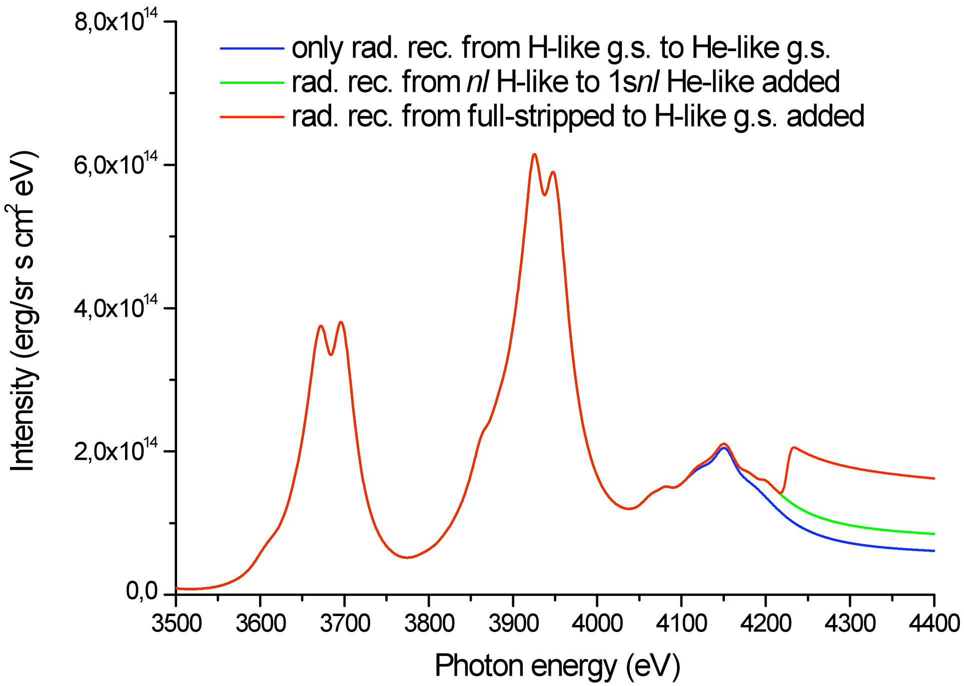

Results

- Determination of the time-histories of the spatially-averaged electron temperature and density in the core has been used to show the influence of high- and low-adiabat laser pulse shapes on the implosion dynamics.

- For that purpose:

- Atomic energy structure from C-like to H-like Ar, including autoionizing and non-autoionizing states and following a relativistic DCA approach, was calculated with FAC [11].
- We used ABAKO to compute a database of emergent intensities in the photon energy range from 3000 eV to 4300 eV over a 30x65 grid of T_e (from 500 to 2250 eV) and N_e (from 3×10^{22} to 5×10^{24} cm^{-3}) values.
- Extraction of Te and Ne for a given spectral lineout is performed by searching in the database the synthetic spectrum that yields the best fit to the data over the optically thin range (from Heβ to Lyγ) on a least-square minimization.

Results

Example of analysis: s49956

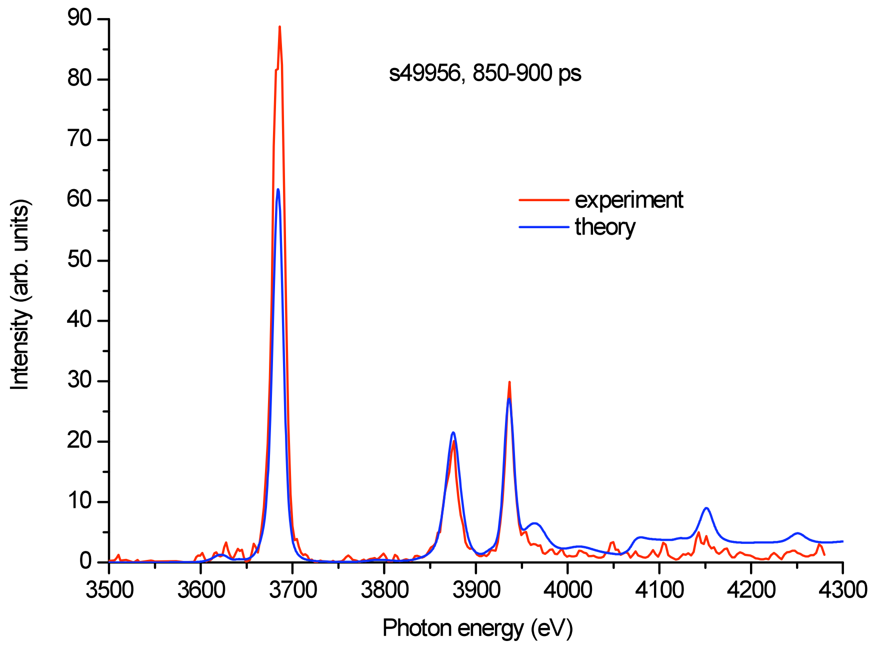

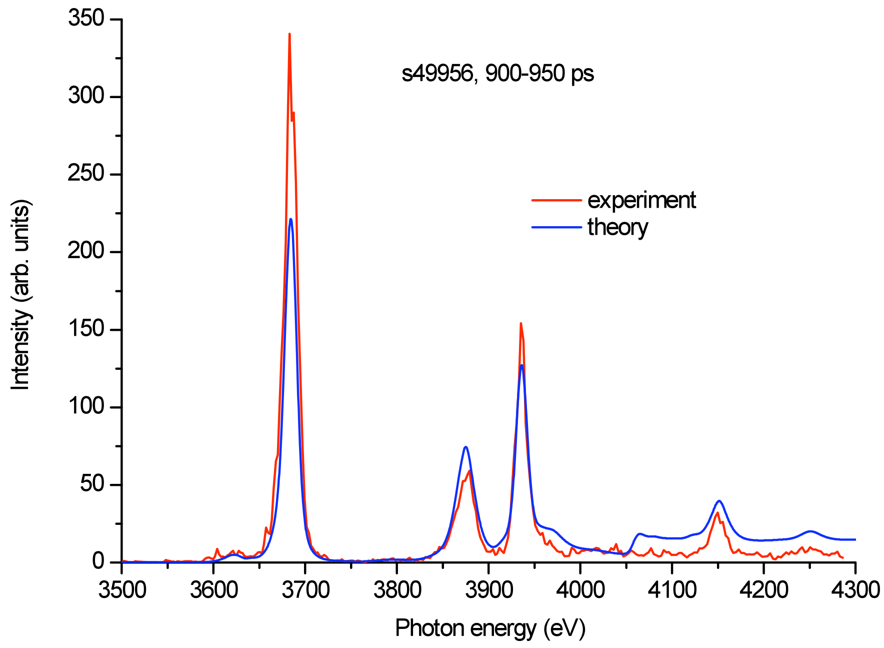

Results

Example of analysis: s49956

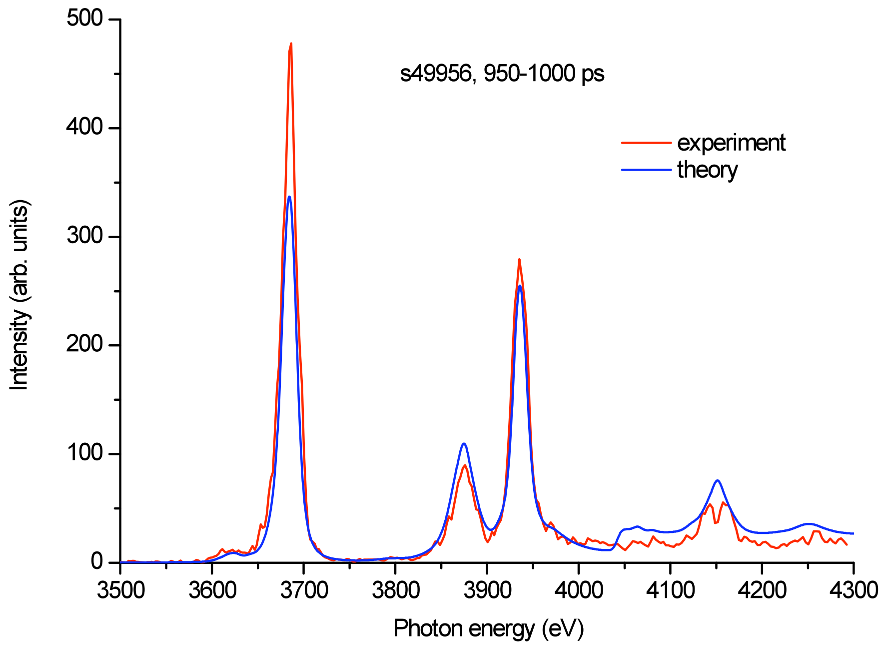

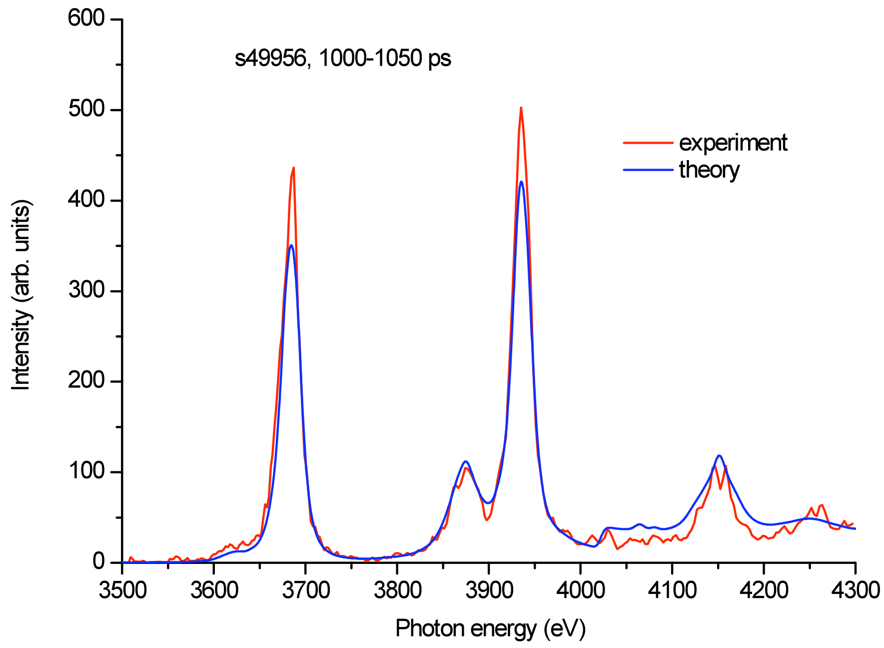

Results

Example of analysis: s49956

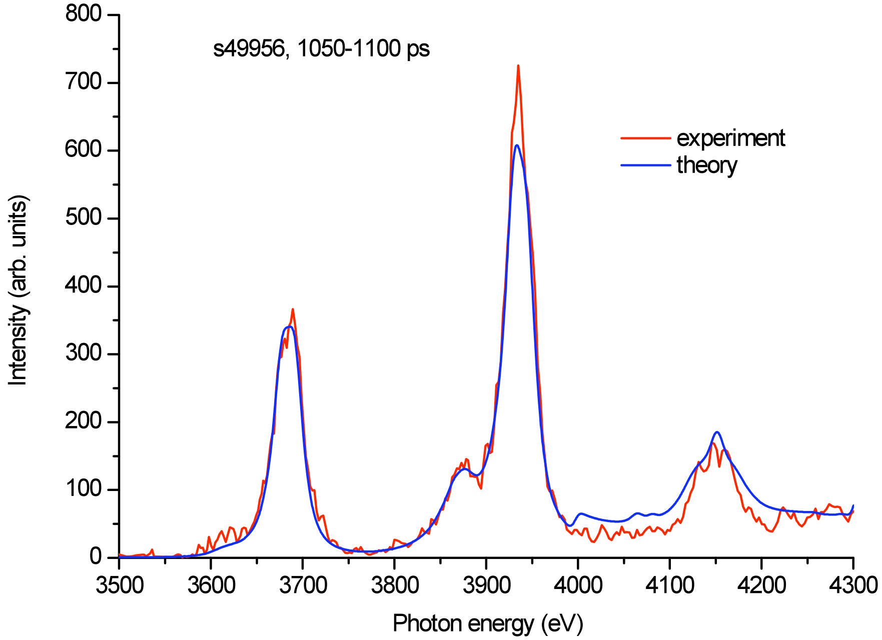

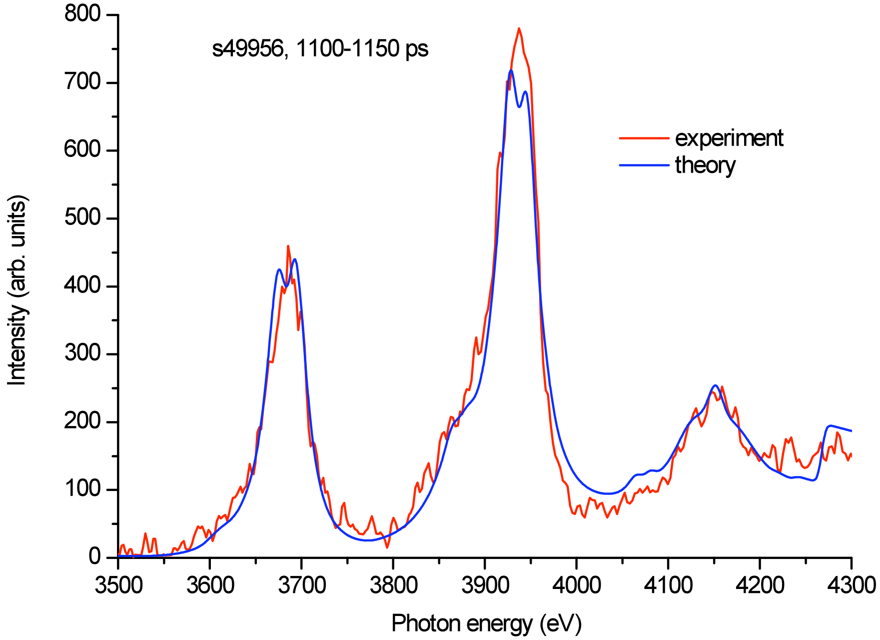

Results

Example of analysis: s49956

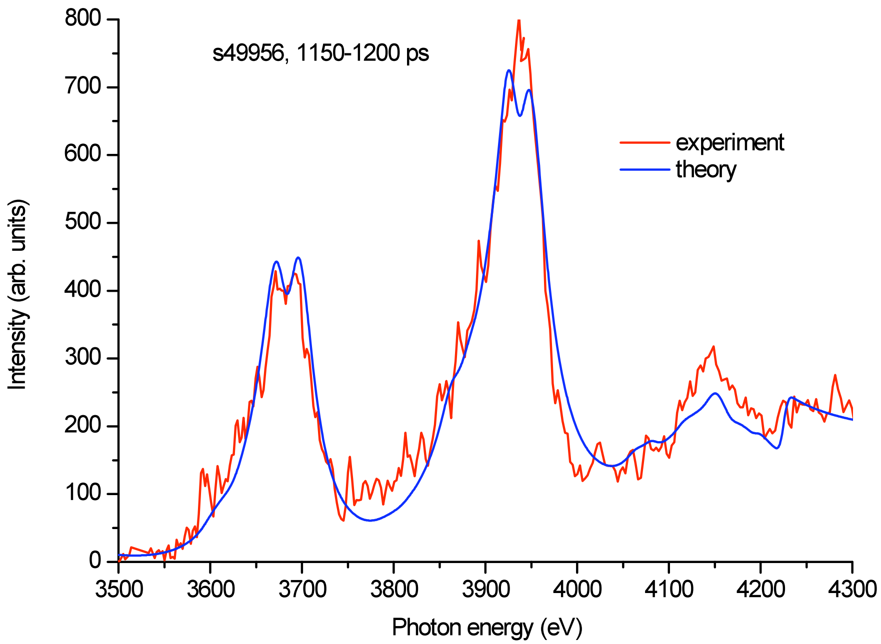

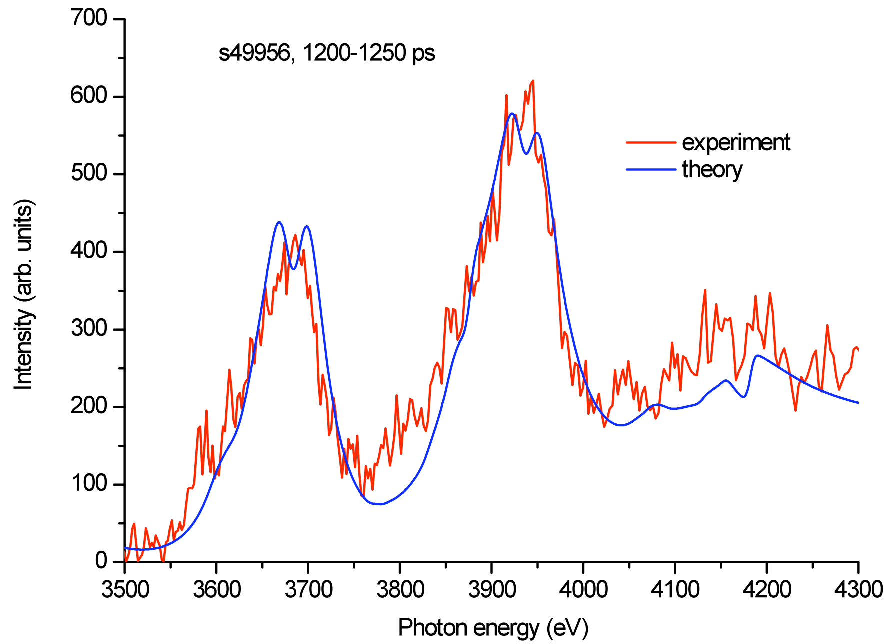

Results

High-adiabat implosion:
electron temperature and density time-histories [12]

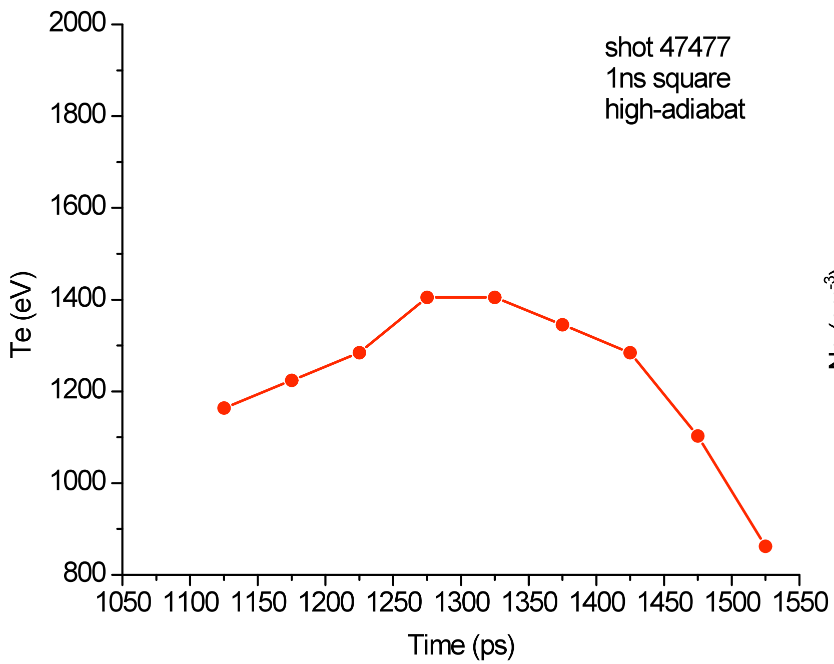

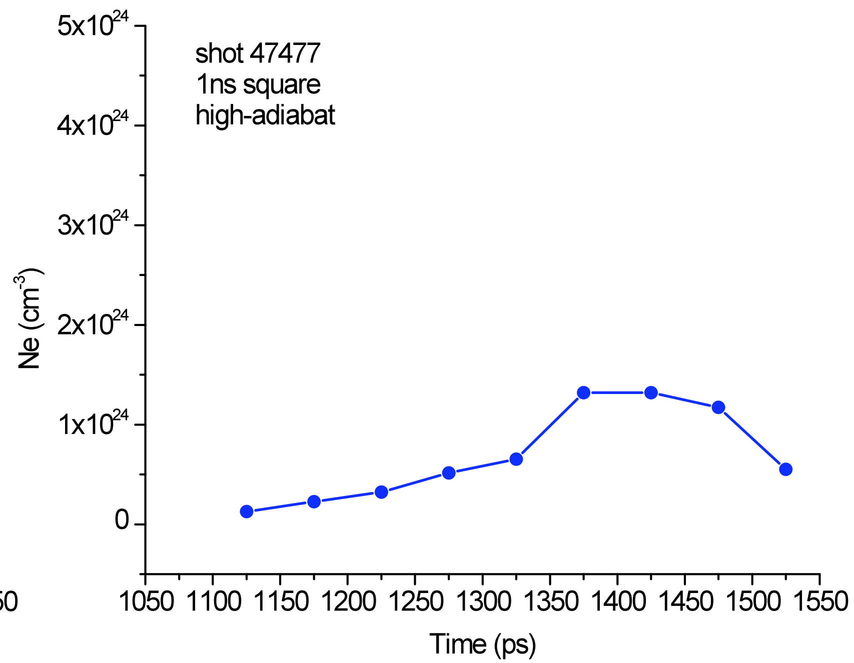

Low-adiabat (α3) implosion: electron temperature and density time-histories [13]

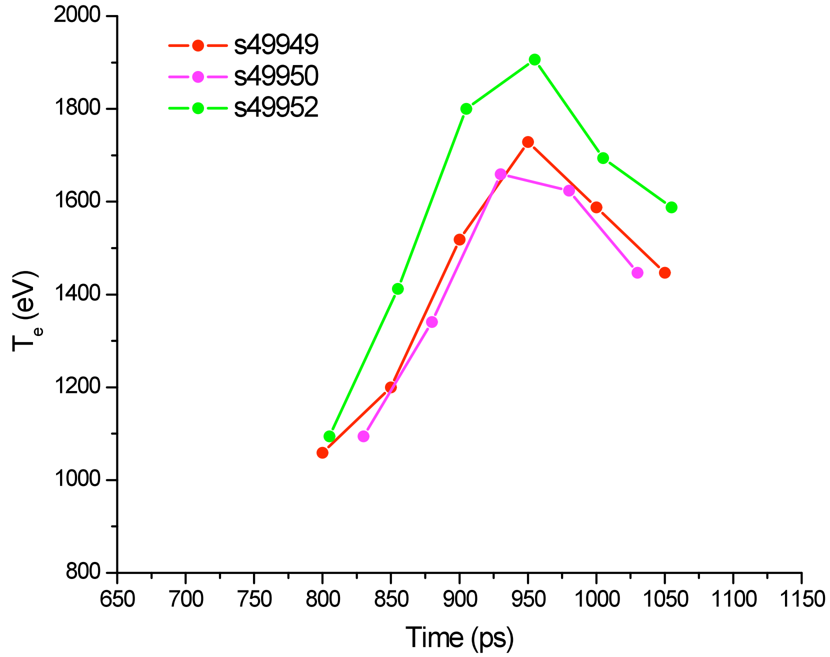

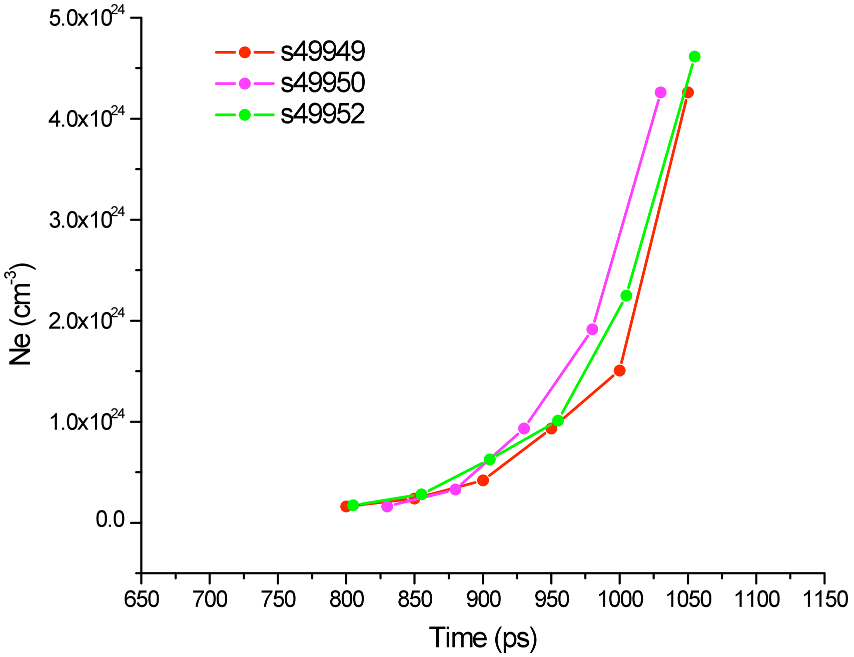

Results

Low-adiabat (α2) implosion: electron temperature and density time-histories [13]

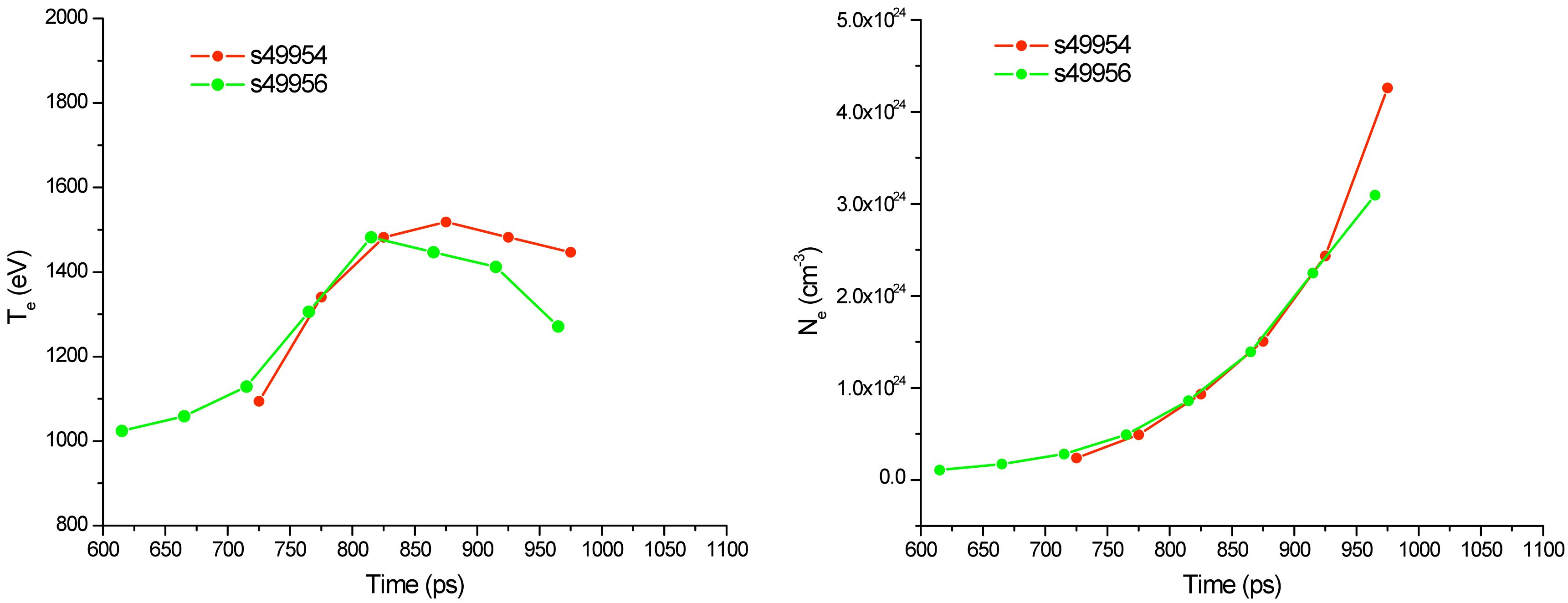

Conclusions

- Time-resolved, space-integrated argon x-ray line spectra have been successfully recorded with SSCA in OMEGA direct-drive, high-adiabat (1ns square) and low-adiabat (α2 and α3) plastic shell implosions, filled with deuterium gas and a tracer amount of argon.
- A detailed spectral model based on the atomic kinetics code ABAKO, Stark-broadened line shapes, and radiation transport calculations was used to analyze the data.
- The analysis of the time-resolved spectra yields the time-histories of the spatially-averaged electron temperature and density in the core through the collapse of the implosion.
- The spectroscopic analysis results show significant differences in core hydrodynamic behavior through the implosion collapse.

This work is supported by DOE NLUF grant DE-FG-07NA28062, and LLNL

References

[1] S. P. Regan *et al.* Phys. Plasmas **9**, 1357 (2002).

[2] L. Welser *et al.* J. Quant. Spectrosc. Radiat. Transf. **81**, 487 (2003).

[3] R. Florido. Ph.D. thesis, Universidad de Las Palmas de Gran Canaria (2007).

[4] H. R. Griem. *Principles of plasma spectroscopy.* Cambridge University Press (1998).

[5] R. C. Mancini *et al. J. Phys. B: At. Mol. Phys.* **20**, 2975-2987 (1987).

[6] R. More. *Atomic physics in inertial confinement fusion*, UCRL-84991, LLNL (1981).

[7] M. S. Dimitrijevic, N. Konjevic. Astron. Astrophys. **172**, 345 (1987).

[8] R. C. Mancini *et al.* Comp Phys Commun **63**, 314 (1991).

[9] D. A. Haynes Jr *et al.* Phys. Rev. E **53**, 1042 (1996).

[10] T. Burris-Mog *et al.* J. Quant. Spectrosc. Radiat. Transf. **99**, 120 (2006).

[11] M. F. Gu. Astrophys. J. **582**, 1241 (2003).

[12] R. Florido, T. Nagayama, R. C. Mancini et al, Rev. Sci. Instrum. **79**, 10E310 (2008).

[13] R. Florido, R. C. Mancini, T. Nagayama et al (in preparation for publication).